

# Radiomics as an Alternative to T2\* value in Cardiac Iron Overload Staging: A Pilot Study Using Open Access Data.

Silva, KNS<sup>1</sup>, Hewadikaram, EHADK<sup>1</sup>, Rathnayaka, MB<sup>2\*</sup>

<sup>1</sup>Department of Electrical, Electronic and Telecommunication Engineering, General Sir John Kotelawala Defence University, Sri Lanka, <sup>2</sup>Department of Nuclear Science, University of Colombo, Sri Lanka

## Introduction

Thalassemia is a hereditary blood disorder that leads to severe anemia, requiring regular blood transfusions as a primary treatment.[1-3] However, repeated transfusions result in cardiac iron overload (CIO), a critical complication causing cardiomyopathy, arrhythmias, and heart failure, which is a leading cause of mortality in thalassemia major. Early detection of CIO is crucial but remains challenging due to the limitations of existing diagnostic methods like serum ferritin measurement, endomyocardial biopsy, and T2\*-weighted MRI, which face issues of invasiveness, cost and technical constraints. This study addresses these gaps by proposing a radiomics-based, noninvasive approach for CIO detection and staging, using high-dimensional quantitative imaging features and machine learning algorithms for accurate and early diagnosis, enabling better clinical outcomes.

## Methods

This study utilized the CHMMOTv1 [4] dataset comprising 124 thalassemia patients, focusing on T2\* and R2\* to classify CIO into Normal (T2\*>20 ms), Moderate (20 ms>T2\*>10 ms), and Severe (T2\*<10 ms) categories. For the current study 42 subjects were randomly selected, covering all three stages. Regions of interest (ROIs) were segmented (Figure 1- (a) and (b)) from cardiac MRI images (TE/TR 3.2 ms/31.3 ms, matrix size = 128×116, slice thickness = 10 mm, FOV = 40×40 cm) using 3D Slicer software. Using the pyRadiomics Python library, a total of 856 radiomic features were extracted. These features encompass various categories, including first-order statistics, texture features, shape descriptors, and wavelet-transformed features. Feature selection techniques—Random Forest (RF), Recursive Feature Elimination (RFE), Lasso Regression, and Boruta—used to identify the top 10 most relevant features for classification. Machine learning models RF, support vector machine (SVM) and Extreme Gradient Boosting (XGBoost) were trained on these features. Class imbalance was addressed using the Synthetic Minority Oversampling Technique (SMOTE)[5]. Model performance was evaluated using accuracy, F1 score, and AUC-ROC, ensuring the identification of the best classifier for CIO detection.

## Results

Feature selection techniques, including RF, RFE, Lasso Regression, and Boruta, successfully identified the top 10 most relevant features. Among these, texture and shape features stood out as critical biomarkers for classification. The study demonstrated the effectiveness of radiomics features and machine learning model in classifying cardiac iron overload (CIO) severity levels in thalassemia patients. Among the tested models, XGBoost [6-8] achieved the best performance with an accuracy of 91%, an F1 score of 0.92, and an AUC-ROC of 1.00, (Figure 2 – (a) and (b)) showing superior capability in distinguishing Normal, Moderate, and Severe categories. RF performed reasonably well, with an accuracy of 73% and an F1 score of 0.74, but struggled with the Moderate class due to overlapping feature distributions. SVM displayed lower effectiveness.

## Discussion

The findings highlight the potential of radiomics and machine learning for non-invasive detection of CIO. XGBoost's ability to handle complex data interactions and high-dimensional datasets made it the preferred model for this application. The study also emphasized the significance of texture and shape features in capturing structural and textural alterations in cardiac tissues due to iron deposition. However, challenges such as the small dataset size and class imbalance impacted the differentiation of Moderate and Severe categories. Future efforts should focus on employing deep learning techniques, such as convolutional neural networks (CNNs), for automated feature extraction and integrating

radiomics features with clinical parameters like serum ferritin and T2\* relaxation times. These advancements could enhance model robustness, improve diagnostic accuracy, and support the development of a standardized multi-modal tool for early detection and personalized management of CIO in thalassemia patients.

## Conclusion

Our clustering-based analysis of Multiparametric-MRI demonstrates that high-intensity clusters of Ktrans, Ve, mean Ktrans and mean Kep are statistically significant parameters for differentiating TP from PsP. Tumor volume difference between TP and PsP was near significant (p=0.07), suggesting that TP is associated with more severe tumor profile. These findings support using DCE-MRI and clustering techniques as non-invasive tools for distinguishing TP from PsP. Future studies should validate these results with larger datasets and integrate more comprehensive multimodal imaging data.

## References

- [1] G. Bartoloni, F. Italia, G. Ferraro, T. Lombardo, C. Tamburino, and S. Cordaro, 'Histopathology of Thalassemic Heart Disease: An Endomyocardial Biopsy Study', *Cardiovascular Pathology*, vol. 6, no. 4, pp. 205–211, Jul. 1997, doi: 10.1016/S1054-8807(96)00136-6.
- [2] E. C. Chapchap et al., 'Alpha- and Beta-thalassemia: Rapid Evidence Review', *Am Fam Physician*, vol. 105, no. 3, pp. 272–280, Mar. 2022, doi: 10.1016/j.htct.2021.01.014.
- [3] H. L. Muncie and J. S. Campbell, 'Alpha and Beta Thalassemia', 2009. [Online]. Available: www.aafp.org/afp.
- [4] I. Abedi, M. Zamanian, H. Bolhasani, and M. Jalilian, 'CHMMOTv1 - cardiac and hepatic multi-echo (T2\*) MRI images and clinical dataset for Iron overload on thalassemia patients', *BMC Res Notes*, vol. 16, no. 1, pp. 1–5, Dec. 2023, doi: 10.1186/S13104-023-06707-5/FIGURES/3.
- [5] R. Blagus and L. Lusa, 'SMOTE for high-dimensional class-imbalanced data', *BMC Bioinformatics*, vol. 14, no. 1, pp. 1–16, Mar. 2013, doi: 10.1186/1471-2105-14-106/FIGURES/7.
- [6] A. Ogunleye and Q. G. Wang, 'XGBoost Model for Chronic Kidney Disease Diagnosis', *IEEE/ACM Trans Comput Biol Bioinform*, vol. 17, no. 6, pp. 2131–2140, Nov. 2020, doi: 10.1109/TCBB.2019.2911071.
- [7] D. Nielsen, 'Tree Boosting With XGBoost Why Does XGBoost Win "Every" Machine Learning Competition?'
- [8] T. Chen and C. Guestrin, 'XGBoost: A scalable tree boosting system', *Proceedings of the ACM SIGKDD International Conference on Knowledge Discovery and Data Mining*, vol. 13-17-August-2016, pp. 785–794, Aug. 2016

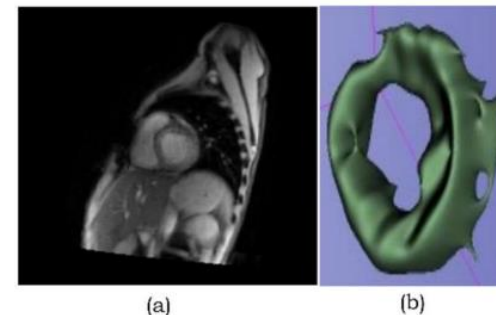


Figure 1- (a) cardiac MRI image from the database, (b) segmented myocardium

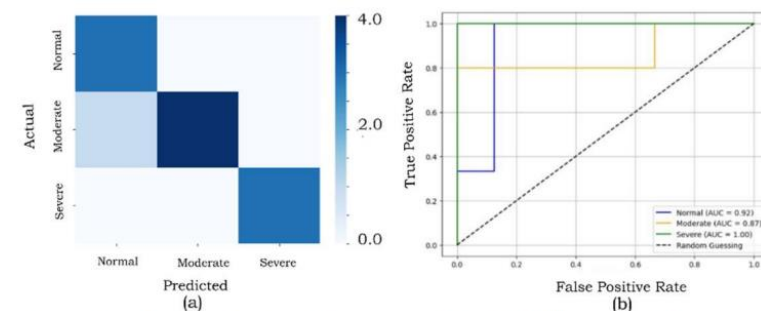


Figure 2 - (a) Confusion matrix for XGBoost classifier, (b) ROC AUC curve for XGBoost classifier